

The strategic dual image method for the open boundary electromagnetic field problems

K. Takahashi^a, Y. Saito^b and S. Hayano^b

^aHitachi Research Laboratory, Hitachi Ltd., Hitachi, Ibaraki 319-12, Japan

^bCollege of Engineering, Hosei University, 3-7-2 Kajino, Koganei, Tokyo, 184, Japan

Received 23 January 1992

We have previously proposed a strategic dual image method for solving open boundary electromagnetic field problems. Now, a new implementation technique for the method is presented to solve saturable and dynamic open boundary electromagnetic field problems in a systematic manner.

1. Introduction

An inherent characteristic of electromagnetic field problems having open boundaries makes it difficult to obtain a finite element or difference solution. Various means have been proposed to get solutions, such as infinite element, balloning and infinitesimal scaling methods [1–3]. Additionally, we have previously proposed a strategic dual image method, which is based on the essential nature of vector fields, i.e. any vector field is composed of rotational and divergence field components [4–6]. In that method, the rotational and divergence field components of an open electromagnetic field are separated by imposing the images of rotational and divergence field sources, respectively. The rotational and divergence field components are obtained by imposing, respectively, zero and symmetrical boundary conditions onto a hypothetical boundary when the field is represented in terms of the vector potentials. Combination of both rotational and divergence field components yields the open boundary electromagnetic fields. Thus, the strategic dual image method makes it possible to obtain the finite element and difference solutions

of the open boundary problems without using any other approaches such as an integral method.

A new implementation technique of the strategic dual image method is presented here to solve saturable and dynamic open boundary electromagnetic field problems systematically. Several examples concerned with the dynamic, saturable and axisymmetric field problems suggest that most of the open boundary electromagnetic field problems can be solved by means of the conventional finite element method.

2. The strategic dual image method

2.1. Principle

In most fields appearing in physical systems, the field intensity decreases on moving away from the source point. In addition to this field intensity decrease, the potential may be reduced to zero, so that both the field intensity and potential become zero at an infinitely long distance from the source point. This means the symmetrical and zero boundary conditions held at the infinitely long distance.

A key feature of the strategic dual image method is that any open boundary solution vec-

Correspondence to: Dr. K. Takahashi, Hitachi Research Laboratory, Hitachi Ltd., Hitachi, Ibaraki 319-12, Japan.

tor in the electromagnetic field problems can be obtained by averaging the symmetrical and zero boundary solution vectors. These symmetrical and zero boundary solution vectors are respectively evaluated by imposing the symmetrical and zero boundary conditions onto a hypothetical boundary located at a finite distance from the source point. Establishment of the symmetrical and zero boundary conditions at the hypothetical boundary is carried out by assuming strategic dual images.

This method is sufficient to understand that the symmetrical and zero boundary solutions give the upper and lower bounds of the open boundary solution, respectively.

2.2. Implementation

Let us assume a discretized system of the equation:

$$CX = F, \quad (1)$$

where C , X and F are the system matrix, solution vector and input vector, respectively; and the symmetrical boundary condition at the hypothetical boundary is assumed. Equation (1) is rewritten as

$$\begin{bmatrix} C_{11} & C_{12} \\ C_{21} & C_{22} \end{bmatrix} \begin{bmatrix} X_{1s} \\ X_{2s} \end{bmatrix} = \begin{bmatrix} F_1 \\ 0 \end{bmatrix}, \quad (2)$$

where X_{1s} is a sub-vector on the inside region; X_{2s} is a sub-vector on the hypothetical boundary; F_1 is an input vector on the inside region; the subscript s refers to the symmetrical boundary solution; and sub-matrices C_{11} , C_{12} , C_{21} , C_{22} are correspondingly defined to X_{1s} , X_{2s} , respectively; and the zero boundary condition at the hypothetical boundary is assumed. Equation (1) is rewritten again as

$$C_{11}X_{1z} = F_1, \quad (3)$$

where the subscript z refers to the zero boundary solution.

Equations (2) and (3) can be written in the following form

$$\begin{bmatrix} C_{11} & C_{12} & 0 \\ C_{21} & C_{22} & 0 \\ 0 & 0 & C_{11} \end{bmatrix} \begin{bmatrix} X_{1s} \\ X_{2s} \\ X_{1z} \end{bmatrix} = \begin{bmatrix} F_1 \\ 0 \\ F_1 \end{bmatrix}. \quad (4)$$

When the open boundary solution vectors are denoted as X_1 for the inside region and X_2 for the hypothetical boundary regions, then the following relationship is established:

$$\begin{bmatrix} X_1 \\ X_2 \\ X_{1z} \end{bmatrix} = \begin{bmatrix} 1/2 & 0 & 1/2 \\ 0 & 1/2 & 0 \\ 0 & 0 & 1 \end{bmatrix} \begin{bmatrix} X_{1s} \\ X_{2s} \\ X_{1z} \end{bmatrix} \quad (5a)$$

or

$$\begin{bmatrix} X_{1s} \\ X_{2s} \\ X_{1z} \end{bmatrix} = \begin{bmatrix} 2 & 0 & -1 \\ 0 & 2 & 0 \\ 0 & 0 & 1 \end{bmatrix} \begin{bmatrix} X_1 \\ X_2 \\ X_{1z} \end{bmatrix}. \quad (5b)$$

By means of eq. (5b), eq. (4) is modified to

$$\left\{ C^T \begin{bmatrix} C_{11} & C_{12} & 0 \\ C_{21} & C_{22} & 0 \\ 0 & 0 & C_{11} \end{bmatrix} C \right\} \begin{bmatrix} X_1 \\ X_2 \\ X_{1z} \end{bmatrix} = C^T \begin{bmatrix} F_1 \\ 0 \\ F_1 \end{bmatrix} \quad (6a)$$

or

$$\begin{bmatrix} 2C_{11} & 2C_{12} & -C_{11} \\ 2C_{21} & 2C_{22} & -C_{21} \\ -C_{11} & -C_{12} & C_{11} \end{bmatrix} \begin{bmatrix} X_1 \\ X_2 \\ X_{1z} \end{bmatrix} = \begin{bmatrix} F_1 \\ 0 \\ 0 \end{bmatrix}, \quad (6b)$$

where

$$C = \begin{bmatrix} 2 & 0 & -1 \\ 0 & 2 & 0 \\ 0 & 0 & 1 \end{bmatrix}. \quad (7)$$

In eq. (6b), if we introduce the relation, $X_{1z} = X_1 + C_{11}^{-1}C_{12}X_2$, then a system of equations for the open fields is given by

$$\begin{bmatrix} C_{11} & C_{12} \\ C_{21} & 2C_{22} - C_{21}C_{11}^{-1}C_{12} \end{bmatrix} \begin{bmatrix} X_1 \\ X_2 \end{bmatrix} = \begin{bmatrix} F_1 \\ 0 \end{bmatrix}. \quad (8a)$$

When ferromagnetic materials are included in the problem region, then their permeabilities are taken into account in the system matrix using [6]:

$$\begin{bmatrix} C_{11} & C_{12} \\ C_{21} & 2C_{22} - C_{21}C_{11}^{-1}C_{12} \end{bmatrix} \begin{bmatrix} X_1 \\ X_2 \end{bmatrix} = \begin{bmatrix} F_1 + (C_{11} - C'_{11})X_1 \\ 0 \end{bmatrix} \quad (8b)$$

or

$$\begin{bmatrix} C'_{11} & C_{12} \\ C_{21} & 2C_{22} - C_{21}C_{11}^{-1}C_{12} \end{bmatrix} \begin{bmatrix} X_1 \\ X_2 \end{bmatrix} = \begin{bmatrix} F_1 \\ 0 \end{bmatrix}, \quad (8c)$$

where C'_{11} is the sub-matrix taking into account the permeabilities of ferromagnetic materials.

2.3. 1D open field

Most one-dimensional (1D) electromagnetic field problems cannot be used practically, but they offer the best examples to illustrate the basic idea of the strategic dual image method.

In fig. 1(a), for a source electric charge Q and its image $+Q$ located at $x = 2L$, a symmetrical boundary condition at $x = L$ can be established. Similarly, imposing a dual image $-Q$ at $x = 2L$ yields a zero boundary condition at $x = L$. The average of both fields in figs. 1(a) and (b) gives an open field caused by the source charge Q . Thus, the open boundary solution vector can be obtained by averaging the symmetrical and zero boundary solution vectors.

2.4. 2D/3D open field

At first, let us consider one of the currents i in the problem region. When an image current $-(d/a)i$ is imposed at the position shown in fig. 2(a), the normal component of flux density B becomes zero at the circular/spherical hypothetical boundary. This means that the vector potential A is zero at the hypothetical boundary when the magnetic field is represented in terms of A . Also, this zero boundary condition $A = 0$ corresponds to the symmetrical boundary condition $\partial U / \partial n = 0$ when the magnetic field is represented in terms of the scalar potential U . The magnitude of the image $-(d/a)i$ depends on the position of the field source current i in the hypothetical boundary so that the following condition must be satisfied to reduce the zero net

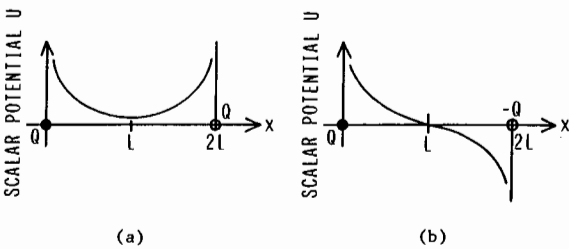


Fig. 1. Strategic 1D dual images: (a) an image charge Q yields a symmetrical boundary at $x = L$; (b) a dual image $-Q$ yields a zero boundary at $x = L$.

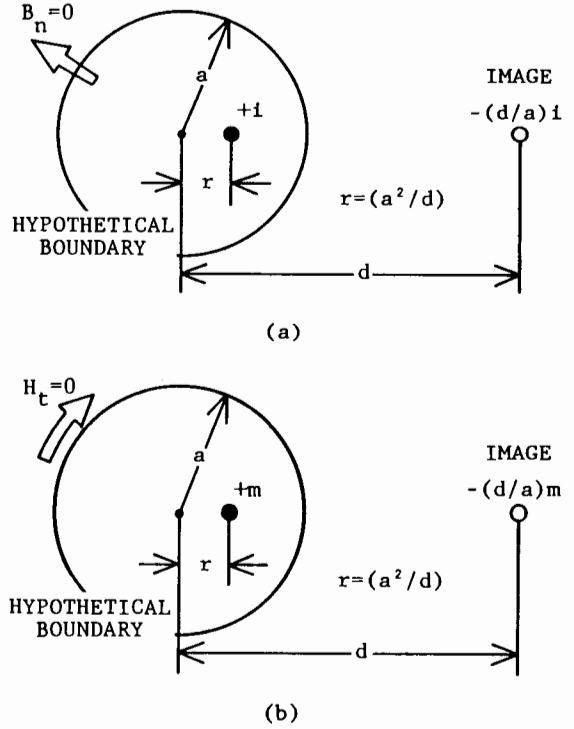


Fig. 2. Strategic 2D/3D dual images: (a) the rotational field source image $-(d/a)i$. The zero $A = 0$ or symmetrical $\partial U / \partial n = 0$ boundary condition is established at the circular/spherical surface; (b) the divergence field source image $-(d/a)m$. The zero $U = 0$ or symmetrical $\partial A / \partial n = 0$ boundary condition is established at the circular/spherical surface.

image:

$$a \sum_{p=1}^q (i_p / r_p) = 0, \tag{9}$$

where a is the radius of the circle/sphere; $r_p (= a^2/d_p)$ is the distance from the center of the circle/sphere to the current i_p ; and q is the number of sources. Equation (4) means that the net current in the problem region must be zero, and the vector potential A becomes zero at the center of the circular/spherical hypothetical boundary.

Secondly, let us consider one of the magnetic charges m in the problem region instead of current i . When an image $-(d/a)m$ is imposed at the position shown in fig. 2(b), the tangential component of the field intensity H becomes zero at the hypothetical boundary. This means that

the scalar potential U is zero at the hypothetical boundary when the magnetic field is represented in terms of U . Also, this zero boundary condition $U=0$ corresponds to the symmetrical boundary condition $\partial A/\partial n=0$ when the magnetic field is represented in terms of the vector potential A .

Thus, the open 2D/3D field solution vector can be obtained by using the circular/spherical hypothetical boundary and averaging the zero and symmetrical boundary solution vectors.

2.5. Axisymmetrical open field

As shown in fig. 3(a), with an arbitrary current i flowing toward the ϕ direction, this problem can be reduced to an axisymmetrical field problem. When we impose an image current $-i$, then, as shown in fig. 3(b), the vector potential A_ϕ becomes zero along an ellipse. This means that the hypothetical boundary of the axisym-

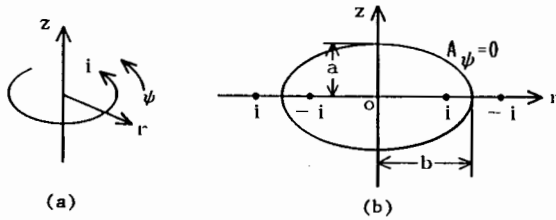


Fig. 3. Axisymmetrical open field: (a) an arbitrary current i flowing toward the ψ direction: (b) a strategic image current and an elliptical hypothetical boundary.

metrical open field becomes an ellipsoid of gyration. Depending on the axial ratio b/a , a large number of ellipses is considered so that it is essential to determine a unique axial ratio b/a . Numerical tests give the unique axial ratio b/a of the ellipsoid as $b/a = 1.815$. This value makes the elliptical hypothetical boundary common to various current distributions.

When we introduce this axial ratio $b/a = 1.815$ into the following demagnetization factor formulae for an ellipsoid of gyration [7]:

$$N_r = \frac{1}{2[(b/a)^2 - 1]} \times \left[\frac{(b/a)^2}{\sqrt{\{(b/a)^2 - 1\}}} \cos^{-1}\left(\frac{a}{b}\right) - 1 \right], \quad (10a)$$

$$N_z = 1 - 2N_r, \quad (10b)$$

then the demagnetization factors N_z of the z -direction and N_r of the r -direction becomes $N_z = 0.5$ and $N_r = 0.25$. This means that the condition $N_z = 2N_r$ must be satisfied to calculate the $(r-\phi-z)$ axisymmetrical three-dimensional fields in the $(r-z)$ two-dimensional space. In others, it may be considered that both of the currents i and $-i$ in the $(r-z)$ coordinate system shown in fig. 3(b) contribute to the r -axis field component. Thus the axial ratio

$$b/a \doteq 1.815 \quad (11)$$

may become a unique value.

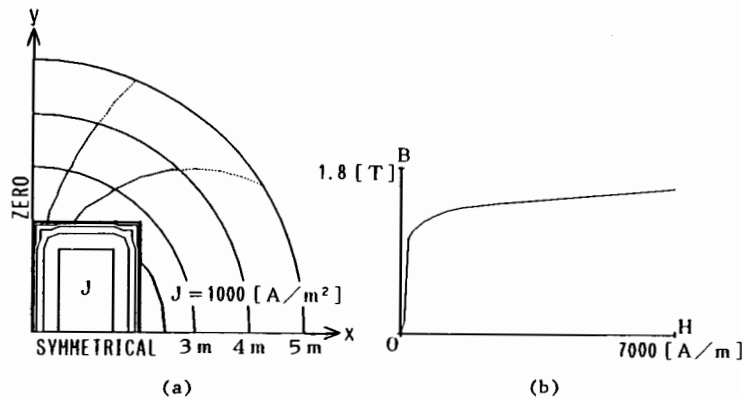
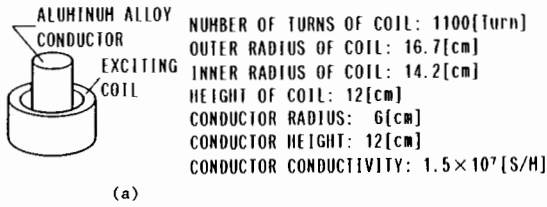


Fig. 4. Magnetic field distribution of a saturable reactor: (a) magnetic field distribution; (b) $B-H$ curve used in the computations.

The axisymmetrical open field vector can be obtained by averaging the symmetrical and zero boundary solution vectors, respectively, while imposing the symmetrical and zero boundary conditions onto the elliptical surface having the axial ratio 1.815.



2.6. Examples

Fig. 4(a) shows the magnetic field distribution in a saturable reactor. Fig. 4(b) shows the $B-H$ curve used in the computation. The solutions are obtained using hypothetical boundaries with different radii. Nevertheless, the solutions almost coincide with each other. This means that the strategic dual image method gives a unique solution, even if nonlinearity of the material is taking into account.

Fig. 5 shows the dynamic field distributions of an axisymmetrical open field. Fig. 6 shows the eddy current distributions in an aluminium alloy conductor. Fig. 7 shows the induced voltages in

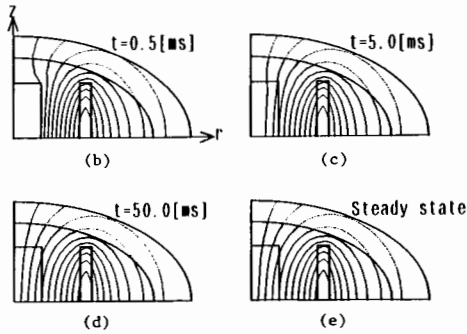


Fig. 5. Axisymmetrical dynamic fields: (a) schematic diagram of the problem; (b)–(e) dynamic field distributions.

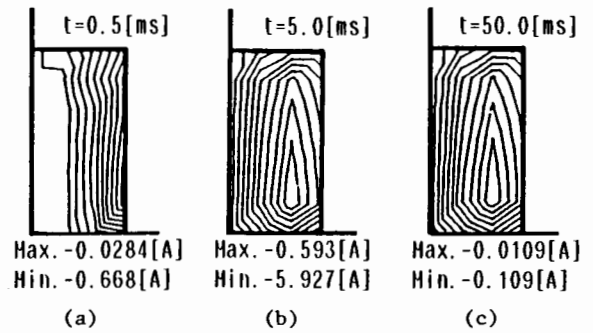


Fig. 6. Eddy current distributions in a conductor.

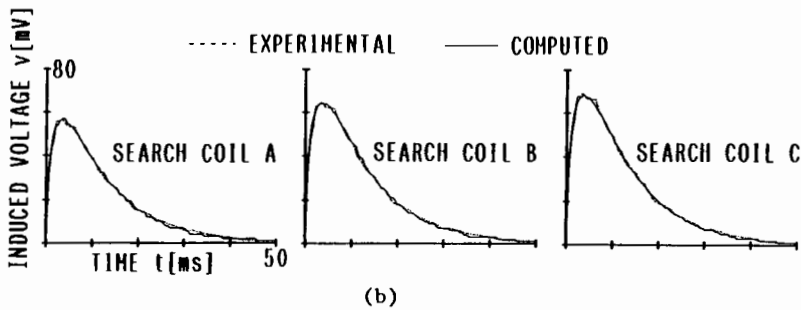
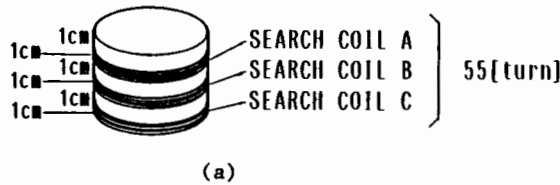


Fig. 7. Experimental verification: (a) search coils attached to a conductor; (b) induced voltages in the search coils together with the experimental results.

search coils together with the experimental results. Agreement between the computed and experimental results in fig. 7(b) suggests that the strategic dual image method is effective for dynamic field problems.

Discretization of the examples in figs. 4–6 is carried out by means of the first-order finite element. Further, the dynamic magnetic fields are obtained by solving the following system equation:

$$\begin{bmatrix} C_{11} & C_{12} \\ C_{21} & 2C_{22} - C_{21}C_{11}^{-1}C_{12} \end{bmatrix} \begin{bmatrix} X_1 \\ X_2 \end{bmatrix} + \begin{bmatrix} D & 0 \\ 0 & 0 \end{bmatrix} \left(\frac{d}{dt} \right) \begin{bmatrix} X_1 \\ X_2 \end{bmatrix} = \begin{bmatrix} F_1 \\ 0 \end{bmatrix}, \quad (12)$$

where a sub-matrix D is due to the conducting medium. Equation (12) is modified to

$$C_1 X_1 + D \left(\frac{d}{dt} \right) X_1 = F_1, \quad (13a)$$

where

$$C_1 = C_{11} - C_{12} [2C_{22} - C_{21}C_{11}^{-1}C_{12}]^{-1} C_{21}, \quad (13b)$$

$$X_2 = -[2C_{22} - C_{21}C_{11}^{-1}C_{12}]^{-1} C_{21} X_1. \quad (13c)$$

The time discretization of eq. (13a) is carried out by means of the backward difference method.

3. Conclusion

The strategic dual image method was demonstrated to make it possible to obtain finite element solutions of open boundary electromagnetic field problems. The procedure was also shown to be extremely simple.

References

- [1] P.P. Silvester and M. Hsieh, Proc. IEE 118 (1971) 1743.
- [2] H. Hurwitz, Jr., IEEE Trans. Magn. MAG-20, (1984) 1918.
- [3] P. Bettess, Int. J. Num. Eng. 11 (1977) 53.
- [4] Y. Saito, K. Takahashi and S. Hayano, IEEE Trans. Magn. MAG-23 (1987) 3569.
- [5] Y. Saito, K. Takahashi and S. Hayano, J. Appl. Phys. 63 (1988) 3366.
- [6] Y. Saito, K. Takahashi and S. Hayano, IEEE Trans. Magn. MAG-24, (1988) 2946.
- [7] K. Ohta, Basic magnetic engineering I, Kyoritsu shuppan, Tokyo (1984).